Article

Development of inclusion complex based on cyclodextrin and oxazolidine derivative

**Rafael Ramos Silva[1], Cézar Augusto da Cruz Amorim[2],
Maria do Carmo Alves Lima[2], Marcelo Montenegro Rabello[1,3],
Marcelo Zaldini Hernandes[1,3], Moacyr Jesus Barreto de Melo Rêgo[1,4],
Maira Galdino da Rocha Pitta[1,4], Maria Danielly Lima de Oliveira[1,5],
César Augusto Souza de Andrade[1,5,*]**

[1]*Programa de Pós-Graduação em Inovação Terapêutica, Centro de Biociências, Universidade
Federal de Pernambuco, Recife, PE, Brasil,* [2]*Laboratório de Química e Inovação Terapêutica,
Departamento de Antibióticos, Universidade Federal de Pernambuco, Recife, PE, Brasil,*
[3]*Laboratório de Química Teórica Medicinal, Universidade Federal de Pernambuco,
Recife, PE, Brasil,* [4]*Laboratório de Imunomodulação e Novas Abordagens Terapêuticas,
Universidade Federal de Pernambuco, Recife, PE, Brasil,* [5]*Laboratório de Biodispositivos
Nanoestruturados, Universidade Federal de Pernambuco, Recife, PE, Brasil*

Oxazolidine derivatives (OxD) have been described as third-line antibiotics and antitumoral agents. The inclusion complexes based on cyclodextrin could improve the solubility and bioavailability of these compounds. A novel synthetic OxD was used, and its inclusion complexes were based on 2-hydroxy-beta-cyclodextrin (2-HPβCD). We conducted an *in silico* study to evaluate the interaction capacity between OxD and 2-HPβCD. Characterization studies were performed through scanning electron microscopy (SEM), Fourier-transformed infrared (FTIR), nuclear magnetic resonance spectroscopy (^{1}H-NMR), X-ray diffraction (XRD), and thermal analyses. A kinetic study of the OxD was performed, including a cytotoxicity assay using peripheral blood mononuclear cells (PBMCs). The maximum increment of solubility was obtained at 70 mM OxD using 400 mM 2-HPβCD. SEM analyses and FTIR spectra indicated the formation of inclusion complexes. ^{1}H-NMR presented chemical shifts that indicated 1:1 stoichiometry. Different thermal behaviors were obtained. The pharmacokinetic profile showed a short release time. Pure OxD and its inclusion complex did not exhibit cytotoxicity in PBMCs. *In silico* studies provided a foremost insight into the interactions between OxD and 2-HPβCD, including a higher solubility in water and an average releasing profile without toxicity in normal cells.

Keywords: Oxazolidine. Cyclodextrin. Solubility. Modeling. Characterization.

INTRODUCTION

Oxazolidine derivatives (OxDs) are synthetic five-ring-membered compounds containing at least one oxygen and nitrogen in their molecular structure. In addition, OxDs have been used as antitumor agents due to their pharmaceutical properties (Alves *et al.*,

2014). A previous study demonstrated that a new OxD presented cytotoxic activity in leukemic lineage cells (HL-60 ATTC®CCL-240) through apoptosis induction mechanisms (Campos *et al.*, 2017). OxDs have an extensive oral application; however, hydrophobic characteristics limit their use *in vivo* (Pandit, Singla, Shrivastava, 2012). Thus, cyclodextrins (CD) have been used as an alternative to increasing solubility through inclusion complexes (Savjani, Gajjar, Savjani, 2012).

CD are cyclic oligosaccharides composed of a hydrophilic outer layer and an internal cavity that can incorporate hydrophobic drugs. These molecules

*Correspondence: C. A. S. Andrade. Laboratório de Biodispositivos Nanoestruturados. Departamento de Bioquímica. Universidade Federal de Pernambuco. CEP: 50670-901, Recife, PE, Brazil. Phone: +55 81 2126.8450. Fax: +55 81 2126.8547. E-mail: csrandrade@gmail.com. ORCID: https://orcid.org/0000-0002-3271-2817

Rafael R. Silva, Cézar A. C. Amorim, Maria C. A. Lima, Marcelo M. Rabello, Marcelo Z. Hernandes,
Moacyr J. B. M. Rêgo, Maira G. R. Pitta, Maria D. L. Oliveira, César A. S. Andrade

offer other advantages, such as pharmacokinetic profile, chemical stability, and low toxicity (Tiwari, Tiwari, Rai, 2010). 2-hydroxylpropyl-β-cyclodextrin (2-HPβCD) is an alternative to α-, β- and γ-CD, with improved water solubility and low toxicological effects (Gould, Scott, 2005). Carvalho et al. (2018) evaluated the inclusion complexes between furazolidone (FZD) and β-cyclodextrin (β-CD), obtaining an increase in the drug solubility and reduction of the toxicity. In addition, *in vitro* evaluations demonstrated FZD:β-CD complexes presented significant improvement in the drug activity.

Furthermore, 2-HPβCD has been pharmaceutically used for parenteral, oral, ophthalmic, and nasal applications (Challa *et al.*, 2005; Rasheed, Ashok Kumar, Sravanthi, 2008). The HPβCD enhances the prodrug penetration associated with a shielding effect from hydrolysis. Bakhtiar, Hop, Walker (1997) showed a similar effect to molecular complexes of an oxazolidine prodrug of (-)-ephedrine, cis-2-(4-methoxyphenyl)-3,4-dimethyl-5-phenyloxazolidine with CD. HPβCD improves the stability of the oxazolidine prodrug toward hydrolysis, increasing therapeutical effects.

The multivariable and complex nature of formulation design seriously hinders product development's efficiency and success rate (Ouyang, Smith, 2015). Thus, molecular modeling of drugs in CD inclusion complexes has been extensively used to predict complexation performance between host: guest molecules (Miletic *et al.*, 2013; Silva *et al.*, 2016; Cavalcanti *et al.*, 2011; Mendonca *et al.*, 2012; Zhao *et al.*, 2019). *In silico* studies involve using theoretical and computational methods that contribute to mimicking the behavior of molecules. One advantage of molecular modeling is to predict the behavior of the guest molecule with a single carrier or host molecule avoiding expensive assays (Alvira, Mayoral, García, 1997; Piel *et al.*, 2001).

In this study, we performed *in silico* analysis and physicochemical characterization to evaluate the interaction energy between a new OxD (5-benzyl-3-ethyl-2-thioxazolidin 4-one) and 2-HPβCD. To the best of our knowledge, no previous work reports the molecular modeling of 5-benzyl-3-ethyl-2-thioxazolidin 4-one (Figure 1) and 2-HPβCD.
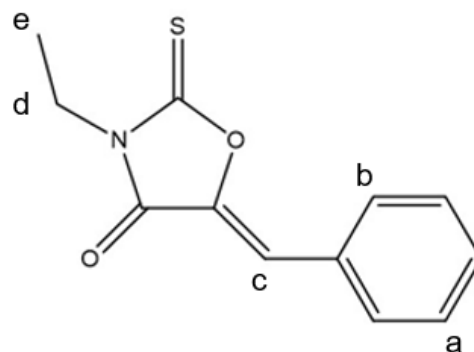
FIGURE 1 - Chemical structure of the new OxD (5-benzyl-3-ethyl-2-thioxazolidin 4-one).

MATERIAL AND METHODS

Material

OxD (5-benzyl-3-ethyl-2-thioxazolidin 4-one) was kindly provided by the Laboratory of Planning and Syntheses of Drugs at the Federal University of Pernambuco (Brazil) (Lima *et al.*, 2015). 2-HPβCD, dimethylsulfoxide (DMSO), DMSO-d6, sodium dodecyl sulfate, acetone, yellow dye 3-(4,5-dimethyl-2- thiazolyl)-2,5-diphenyl-2H-tetrazolium bromide (MTT), glutamine, streptomycin, and penicillin were purchased from Sigma-Aldrich (St. Louis, USA). Deionized (DI) water was obtained from a Milli-Q water purification system (Billerica, MA, USA).

Preparation of OxD:2-HPβCD inclusion complexes

The co-precipitation method was used to obtain inclusion complexes. Initially, OxD and 2-HPβCD at equimolar ratios (1:1) were dissolved in acetone: water (3:1, v/v). OxD solution was dropwise added to the 2-HPβCD solution and maintained under stirring for 6 h. Subsequently, the samples were submitted to rotary evaporation at 45°C for 90 min. After the material had partially dried, the solid was lyophilized (4 × 10^{-6} Barr) for 24 h and stored in desiccators until use. The physical mixture was obtained by mixing OxD and 2-HPβCD at equimolar ratios (1:1) in a mortar and pestle for 10 min to obtain a homogeneous mixture.

Characterization

Morphological analyses were performed using a QUANTA 200 (FEI, OR, USA) scanning electron microscope (SEM) at 30 kV, spot size 3.0, and work distance of ~11.5mm. The images were taken at 500×, 800×, 1,200× and 2,000× magnifications. The samples were placed on aluminum stubs with double-sided carbon tape, and thin gold films were evaporated on the sample surface using a high vacuum film deposition system (SCD 500 Mycrosystems Leica, Wetzlar, DE). Fourier Transform Infrared measurements were evaluated using the KBr pellet method. The baseline correction was performed using a pure KBr disk. Infrared spectra of the OxD and inclusion complexes were recorded using a Vertek 70 Fourier Transform Infrared Spectrophotometer (Bruker, MA, USA) in the range 4000-400 cm^{-1}, wavenumber resolution 2 cm^{-1}, cumulative scans 64 times. ^{1}H- nuclear magnetic resonance (NMR) spectra were recorded on a Varian 400 MHz NMR Spectrometer (Varian, USA) using TMS as internal standard and DMSO-d6 as solvent. The chemical shifts were reported in δ (ppm). XRD diffraction data were collected with a D8 Advance X-ray diffractometer (Bruker, MA, USA) using CuKα radiation in the range of 2□ (30-60)º at 0.03º/second. Simultaneous thermogravimetric (TGA) and differential thermal analysis (DTA) measurements were performed using STA 449 F3 Jupiter® (NETZSCH, Asch, CZ). The measurements were performed under Ar (25 mL min^{-1}) in the temperature range of 40-300ºC at a heating rate of 10º C min^{-1}. DSC thermograms were recorded in the temperature range of 20° to 310°C at a heating rate of 10°C min^{-1}.

Molecular modeling of the OxD: 2-HPβCD inclusion complex

Two chemical aspects of 2-HPβCD were taken into consideration for molecular modeling, as follows: a) Regioselective: the reaction preferably occurs at the primary hydroxyl group OH (6) since these are most accessible, followed by the secondary hydroxyl OH (2) with the highest acidity (pKa=12.2) (Wenz, 1994); b) Homologous derivatives with lower and higher molar substitution ratio (MS) (Treib et al., 1999), which are also formed in the mixture obtained as the final product (Wenz, 1994).

Our approach was to virtually construct 1000 structures (40 configurations with 25 different conformations each) for the 2-HPβCD model, starting from the tridimensional structure of the βCD (Saenger et al., 1998). The 40 configurations were built considering both synthetic aspects mentioned before. Considering the MS of 0.6, it seems reasonable to assume that the 2-HPβCD structure (7 glucose units) has, on average, 4 HP units (0.6×7=4.2). Thus, 20 configurations of 2-HPβCD were built with 4 HP units, ten with 3 HP units, and ten with 5 HP units. For each HP unit added, has been considered the probability of 70% for OH (position 6), 20% for OH (position 2), and 10% for OH (position 3) to select the OH position for substitution. The conformer search was performed using the Genetic Algorithm and Energy Score Function available at the OpenBabel library (O'Boyle et al., 2011), with default convergence parameters. The geometry optimizations for 1000 structures were computed using MMFF94s force field (Halgren, 1999), again with the same library and default criteria.

The Autodock VINA software (Trott, Olson, 2010) was used in the molecular docking approach, considering each entire 2-HPβCD derivative structure as the active site and adjusting the exhaustiveness parameter to 8. The intermolecular interaction energies for all 1000 complexes were calculated. The whole approach for molecular modeling was automated using the CycloMolder platform developed by some of us (Rabello, M.M and Hernandes, M.Z).

Phase Solubility Study of OxD:2-HPβCD

According to Higuchi, Connors (1965), the phase solubility study was carried out to determine the stoichiometric ratio of the host: guest compounds. Six fixed amounts of OxD (1, 10, 25, 50, 75, and 100 µM) were mixed with 2 mL 2-HPβCD aqueous solution and, subsequently, vigorously stirred for 48 h at 25 ºC. After, the samples were centrifuged at 8,972 g for 10 min and filtered with 0.45 µm PVDF membranes

Rafael R. Silva, Cézar A. C. Amorim, Maria C. A. Lima, Marcelo M. Rabello, Marcelo Z. Hernandes, Moacyr J. B. M. Rêgo, Maira G. R. Pitta, Maria D. L. Oliveira, César A. S. Andrade

(Macherey-Nagel, Dueren, DE). The filtered solution was analyzed using an Agilent Cary 60 UV-Vis double beam spectrophotometer at $\square$ = 286 nm. Quartz cells with a 10 mm path length were used. From the slope and intercept value (S_0) of the phase solubility curve, the stability constant ($K_{1:1}$) was determined as follows:

$$K_{1:1} = \frac{slope}{[S_0 \times (1-slope)]} \quad (1)$$

The complexation efficiency (CE) of OxD was determined from data of the phase solubility curve according to the following equation:

$$CE = \frac{slope}{(1-slope)} \quad (2)$$

In vitro release study

In vitro release studies of pure and OxD/2-HPβCD inclusion complexes from the physical mixture and co-evaporation method were performed in triplicate according to Ch.P (2010 Edition, Part 2, Appendix XC. No.2 method) and USP 30-NF 25 (2007 Edition, Volume 1, <711> Apparatus 2) using an Rcz-602 Dissolution Apparatus (Shanghai Huanghai Medicine Checking Instrument Co., Ltd). Briefly, 2 mg of OxD or OxD:2-HPβCD inclusion complexes were added to 250 mL of DI water (37 ± 0.5 ºC) and stirred at 50 rpm. At predetermined time intervals, 5 mL of the previous solution was withdrawn and centrifuged at 12,000 rpm for 5 min. The drug content was measured at $\square$ = 282 nm using UV spectrometry, and the cumulative release rate was calculated at each time interval.

PBMC cytotoxicity assay

Peripheral blood mononuclear cells were obtained from heparinized blood from healthy donors (n = 5). The cells were isolated via a standard density-gradient centrifugation method over Ficoll-Hypaque solution (GE Healthcare). Cells were counted in a Neubauer chamber, and viability was determined by the trypan blue exclusion method. Cells were used only when the viability was > 98%. All donors gave informed consent, and the Human Research Ethics Committee of UFPE approved the study. The cells were cultured in RPMI-1640 medium supplemented with 10 % fetal calf serum, 2 mM glutamine, 100 mg mL^{-1} streptomycin, and 100 U mL^{-1} penicillin at 37ºC with 5 % CO_2. PBMCs were plated in 96-well plates (10^4 cells well^{-1}) during the cytotoxicity assay. After, the OxD compound (1, 10, 25, 50, 75, and 100 µM) was diluted in DMSO solution and added to each well. The cells were incubated for 72 h. The control groups were treated with the same amount of 0.1 % DMSO.

The growth of PBMCs was quantified by the ability of living cells to reduce the MTT to a blue formazan product. After 72 h of incubation, the medium in each well was replaced with a fresh medium (200 µL) containing MTT (0.5 mg mL^{-1}). After 3h, the formazan product of MTT reduction was dissolved in 20 % sodium dodecyl sulfate, and the absorbance of the solution was measured at $\square$ = 570 nm with a multiplate reader (EL808, Biotek, USA). The cytotoxicity was expressed as the concentration inhibiting 50% of cell proliferation (IC50), which is the percentage reduction in cell viability calculated from the ratio between the number of cells treated with OxD, inclusion complexes, and untreated cells (control).

RESULTS AND DISCUSSION

Molecular modeling of the OxD:2-HPβCD inclusion complex

The molecular docking results showed two main orientations regarding the relative position of the guest molecule (OxD) into the host molecule (2-HPβCD). The first one, orientation I, has the 2-thioxo-oxazolidine-4-one ring at the wider rim of the 2-HPβCD, and the other, called orientation II, has the benzene ring at the wider edge. Considering orientation I, the average docking energy for the ten first-best solutions is -5.6 kcal/mol. On the other hand, the average energy of the ten first best solutions for orientation II is -5.4 kcal/mol, therefore less stable. The overall best docking solution for orientation I is shown in Figure 2a, with a docking energy of -5.9 kcal/mol.

In contrast, the best docking solution for orientation II can be found in Figure 2b, with energy of -5.6 kcal/mol. The best docking solution for orientation I is stabilized by several hydrophobic contacts and three hydrogen bonds (2.9 Å, 3.0 Å, and 3.1 Å). At the same time, several hydrophobic contacts stabilize the best solution for orientation II, but only by two hydrogen bonds (2.9 Å and 3.1 Å). The final molecular modeling results show that orientation I is the most stable. A significant ratio for the OxD:2-HPβCD (host: guest) inclusion complex should occur in the mixture. Our results indicated the possibility of incorporating OxD into 2-HPβCD and overcoming its low aqueous solubility. According to previous studies, 2-HPβCD affects the pharmacokinetic profile associated with a short release time and a high amount of mass dissolved in bulk (Cavalcanti *et al.*, 2011; Dahiya, Pathak, 2006).

Orientation I	kcal/mol	Orientation II
-5.9	1º	-5.6
-5.7	2º	-5.5
-5.6	3º	-5.5
-5.6	4º	-5.4
-5.6	5º	-5.4
-5.5	6º	-5.3
-5.5	7º	-5.3
-5.5	8º	-5.3
-5.5	9º	-5.3
-5.5	10º	-5.3
-5.6	Average	-5.4
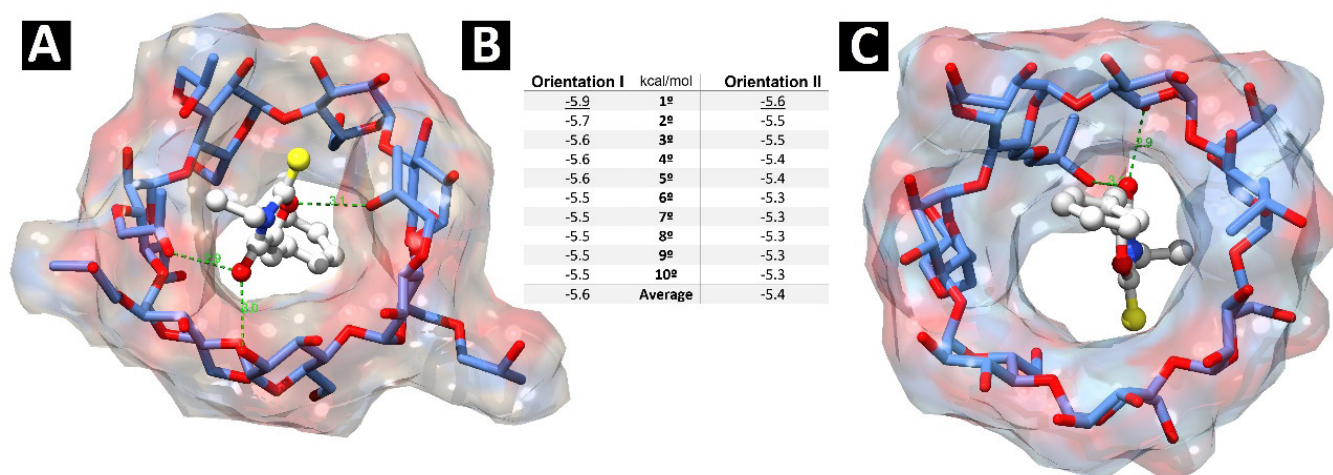
FIGURE 2 - Summary of the molecular docking results. A) Best docking solution for orientation I. B) Binding energy (kcal/mol) table of the ten best docking solutions for each orientation. C) Best docking solution for orientation II. Dashed lines represent intermolecular hydrogen bonds between host (2-HPβCD) and guest (OxD) molecules.

Phase Solubility Study

An A_L-curve type phase solubility diagram was obtained for OxD:2-HPβCD in water (Figure 3). Data were fitted by linear regression leading to the following equation: $[OxD]_{water} = 0.1686 \times [2\text{-HP}\beta CD] + 0.1950$ ($r^2 = 0.98915$). The solubility constants of OxD with 2-HPβCD in water at 25°C were K1:1=0.316 and S_0=0.64mM.

The enhancement of OxD solubility after 2-HPβCD association was obtained initially at 12.62 mM. Of note, a twentyfold increase was obtained over OxD solubility in water (0.64 mM). The CE was calculated according to Eq. 2, and the result was equivalent to 0.202 for OxD. According to Loftsson, Hreinsdóttir, Másson, if CE is 0.1 then 1 of every 11 CD molecules forms a complex with the drug. Our results suggest that approximately 1 of every 5 CD molecules form a complex with OxD (Loftsson, Hreinsdóttir, Másson, 2005).

Rafael R. Silva, Cézar A. C. Amorim, Maria C. A. Lima, Marcelo M. Rabello, Marcelo Z. Hernandes,
Moacyr J. B. M. Rêgo, Maira G. R. Pitta, Maria D. L. Oliveira, César A. S. Andrade
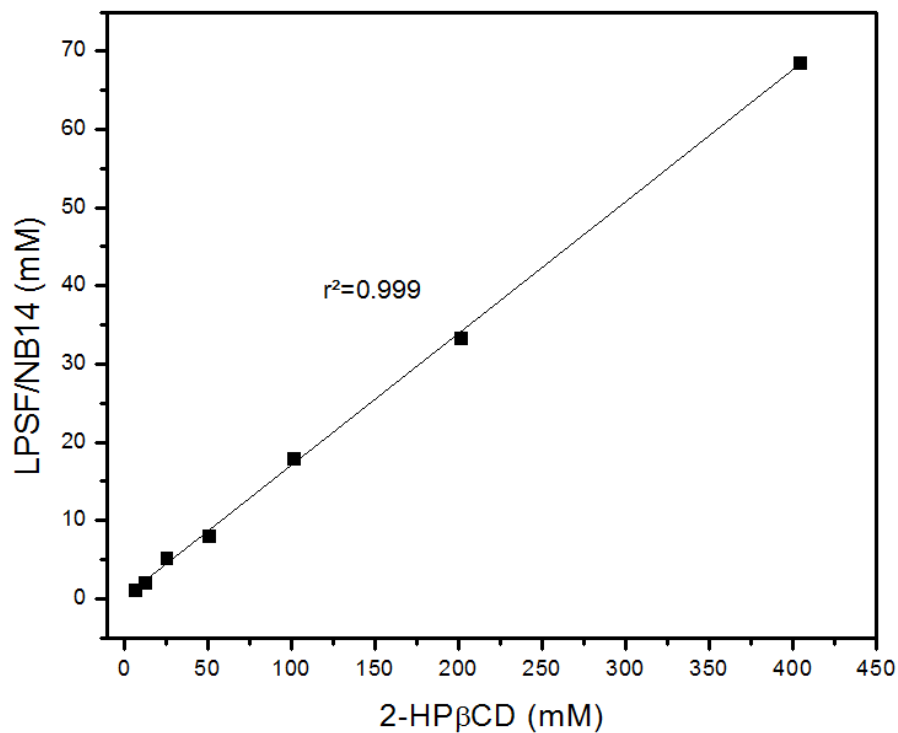
FIGURE 3 - Phase stability diagrams for OxD in the presence of 2-HPβCD at room temperature.

Morphological Analysis

The morphology of OxD and its inclusion complex was evaluated using SEM (Figure 4). OxD image demonstrates a long crystal with a smooth surface presenting an acicular shape (Figure 4a). On the other hand, the inclusion of complex images revealed significant changes in the morphology showing an amorphous form followed by aggregation (Figure 4b). The regular shape of the drug is affected since 2-HPBCD is an amorphous material (Cirri et al., 2005). The morphology of the inclusion complex is similar to other previous studies (Songngam et al., 2014; Fauziah et al., 2013). Our data suggest the incorporation of the OxD in the inner cavity of 2-HPβCD.
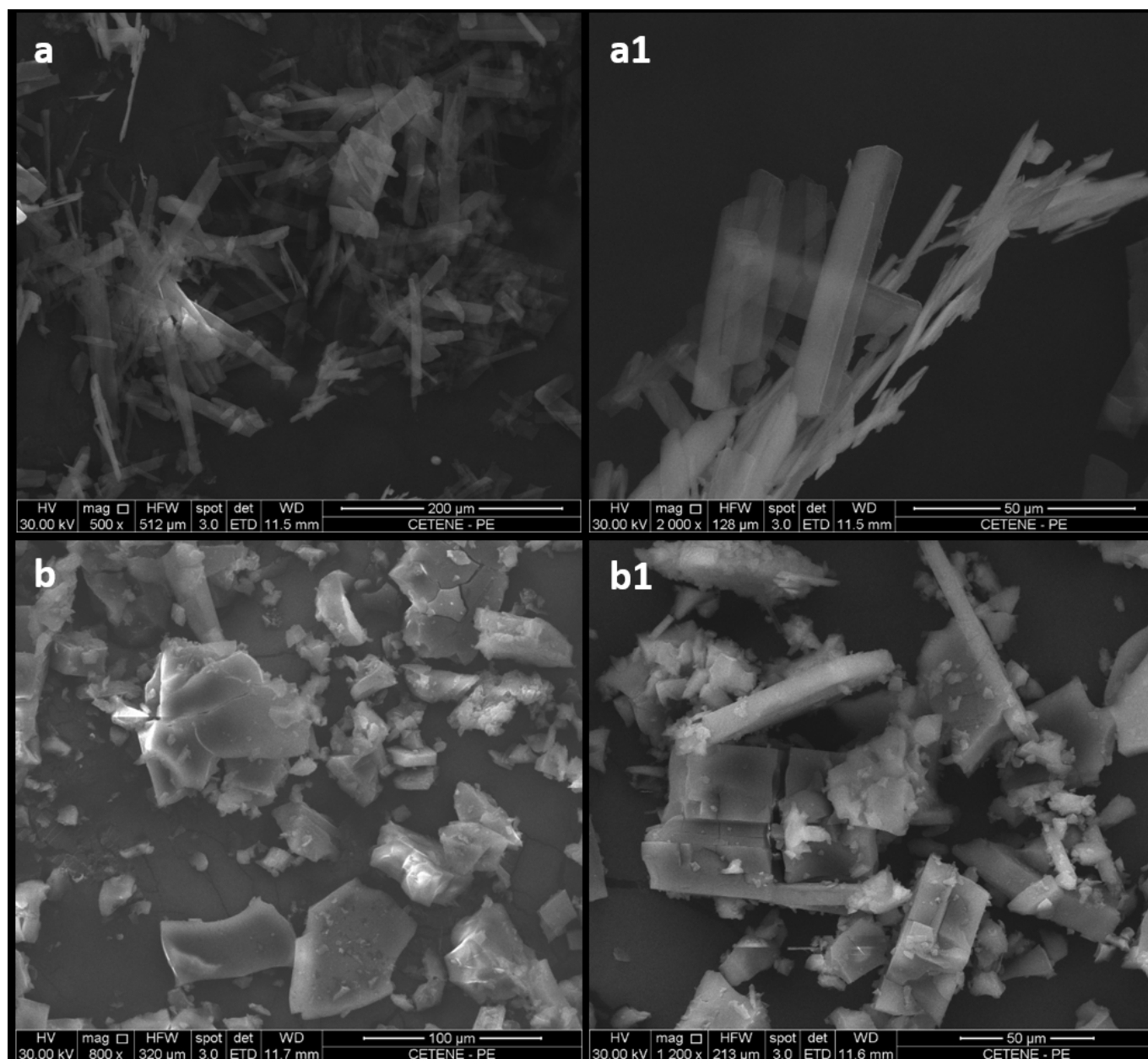
FIGURE 4 - Micrographs of OxD (a and a1) and OxD:2-HPβCD inclusion complex (b and b1).

Fourier transform infrared spectroscopy (FTIR) analysis

FTIR spectra from co-evaporation and physical mixture methods were compared to evaluate the efficiency of these methodologies (Figure 5). FTIR spectrum of OxD showed the presence of bands at 1750-1735 cm⁻¹ (C=O stretch), 1600-1585 cm⁻¹ (C–C stretch, aromatic), 1360-1290 cm⁻¹ (C–N stretch, aliphatic amines) and 1050-1200 cm⁻¹ (C=S stretch, thiocarbonyl). The FTIR spectrum of OxD also shows the presence of bands at ☐3016 (C–H stretching vibration), 1745 and 1695 (C=O stretching), and 1631 cm⁻¹ (C=C stretching). The FTIR spectrum of 2-HPβCD shows prominent absorption bands at ☐3411 (O–H stretching vibration), ☐2931 (C–H stretching vibration), ☐1157, ☐1089, and ☐1029 cm⁻¹ (C−H and C−O stretching vibration). 2-HPβCD presented a considerable overlap of signals, with slight changes

in the intensity and broadenings of the absorption bands, indicating the formation of inclusion complexes with typical fingerprint bands. The results showed the formation of the inclusion complexes, considering the decrease in the intensity of the absorption bands of the OxD functional groups. Our results indicate that the co-evaporation method was more efficient than the physical mixture method.
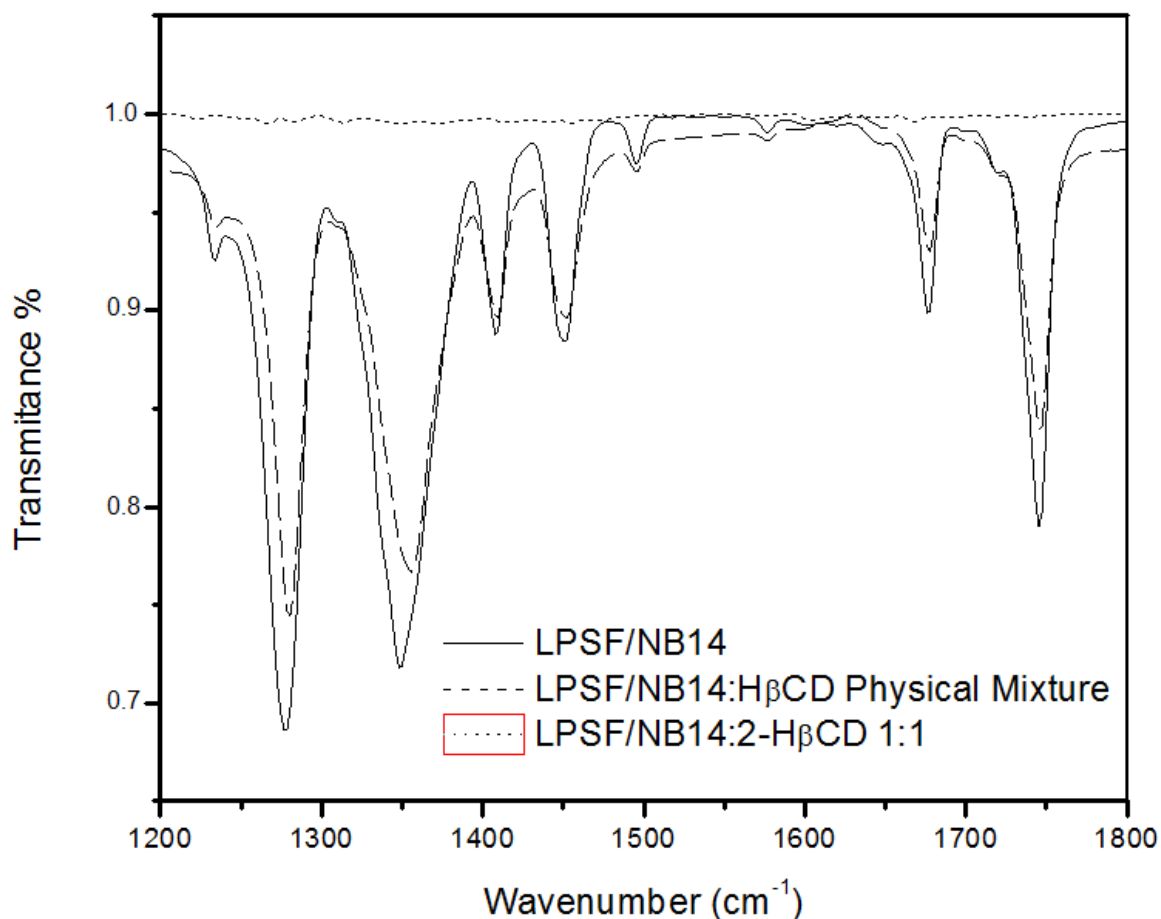
FIGURE 5 - FTIR spectra of OxD and OxD:2-HPβCD inclusion complex by physical mixture and co-evaporation method at 1:1 molar ratio.

Nuclear magnetic resonance spectroscopy (1H-NMR) measurements

^{1}H-NMR experiments were performed to confirm the formation of OxD:2-HPβCD inclusion complex. The pure compounds' chemical shifts ($\Delta\delta$) at a 1:1 molar ratio were evaluated (Table I). The OxD ^{1}H-NMR presented (400 MHz, DMSO-d6): δ=1.220 (t, 3H, CH$_3$, J= 7,2 Hz), 3.918 (q, 2H, CH$_2$, J= 7,2 Hz), 6.942 (s, 1H, =C-H), 7.550 (m, 3H, C-H Ar), 7.881 (d, 2H, J= 8,4 Hz, C-H Ar). The host-guest interaction (OxD:2-HPβCD) resulted in both shifted H$_3$ and H$_5$ protons of the 2-HPβCD ($\Delta\delta$ = 0.011 ppm and 0.009 ppm, respectively) (Table II). Of note, H$_3$ and H$_5$ protons are located inside the hydrophobic cavity of the 2-HPβCD. Thus, our results indicated the potential of 1:1 stoichiometry for OxD interaction in the inner cavity of 2-HPβCD. The chemical shift changes suggest that hydrogen bonds contribute to the insertion of the compound into the CD cavity (Hara *et al.*, 2006).

TABLE I - ¹H-NMR signals of OxD and OxD:2-HPβCD at 1:1 molar ratio

δOxD (ppm)	δOxD:2-HPβCD (ppm)	Δδ (ppm)
7.881	7.879	0.002
7.550	7.549	0.001
6.942	6.941	0.001
1.220	1.217	0.003

TABLE II - ¹H-NMR signals of 2-HPβCD and OxD:2-HPβCD at 1:1 molar ratio

	δHPβCD (ppm)	δOxD:2-HPβCD (ppm)	Δδ (ppm)
H_1 (a)	5.090	5.086	0.004
H_2 (b)	3.614	3.612	0.002
H_3 (c)	3.912	3.901	0.011
H_4 (d)	3.390	3.387	0.003
H_5 (e)	3.646	3.637	0.009

X-ray diffraction measurements

XRD patterns presented two well-defined peaks for OxD (Figure 6) that represent a specific structural order of a crystalline solid. Natural and synthetic CD generally have undefined peaks characterized as amorphous materials (Choe *et al.*, 2003). A decrease in the peak intensity of the inclusion complex is observed, indicating a crystallinity loss.
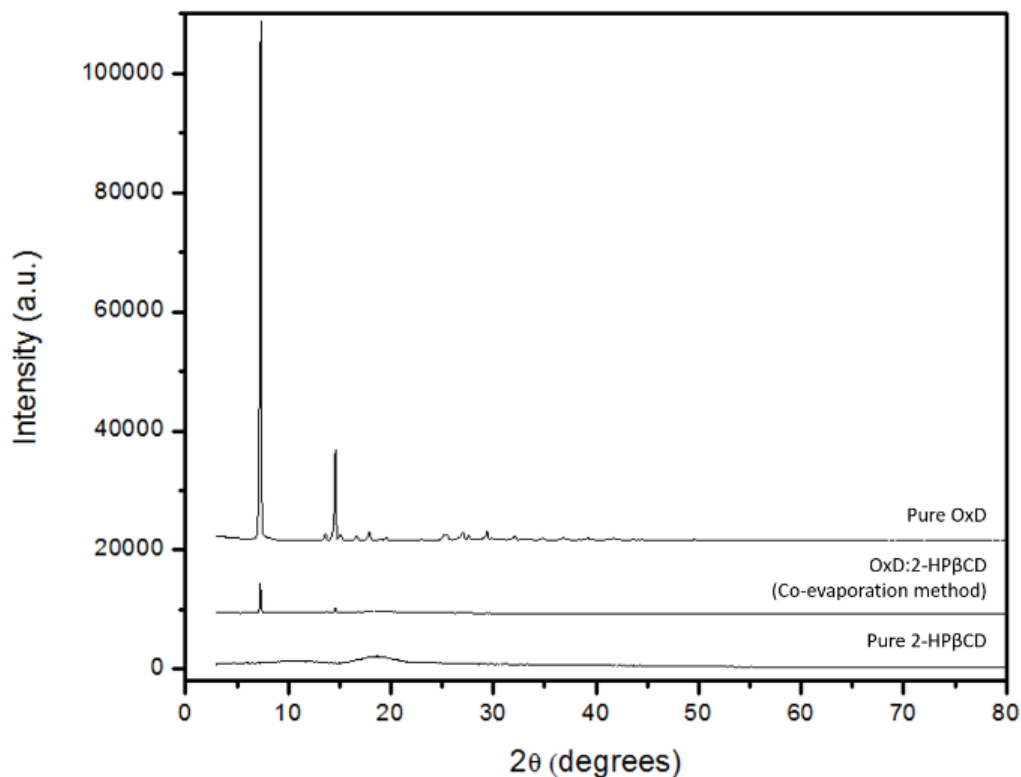
FIGURE 6 - X-ray diffraction patterns of the OxD, 2-HPβCD, and OxD:2-HPβCD inclusion complex.

Thermal Analysis

The thermal behavior of pure compounds and inclusion complexes was evaluated. A significant shift in the thermal behavior was obtained for the inclusion complex (Figure 7a). OxD showed an endothermic peak at 136.57 ºC with a reaction heat of 4.19 J/g that occurs before the decomposition temperature. An exothermic peak at 103.52 ºC with a reaction heat of 1.07 J/g was observed for 2-HPβCD. By following the thermal behavior of the OxD:2-HPβCD inclusion complex, we noticed the presence of an exothermic shift 143.77 ºC with a reaction heats of 0.83 J/g.

Given the analysis of thermogravimetric curves, it is possible to observe a significant mass loss of 27.5% of OxD of about 250-300 ºC. 2-HPβCD showed a discrete mass loss (2.5%) of about 125 ºC and 300 ºC. The mass loss of the inclusion complex was lower than pure OxD

(17.5% *vs.* 27.5%, respectively). These results suggest that 2-HPβCD contributed to a temperature displacement associated with weight loss at higher temperatures (Figure 7b). Then, TG and DSC results demonstrate the effectiveness of the complexation method. In addition, melting point determination is based on intermolecular interactions that stabilize the compound's crystalline structure. Thus, 2-HPβCD cavity offers thermodynamic stability for OxD, resulting in different thermal behavior.

TG and DSC curves of OxD:2-HPβCD inclusion complex exhibited a decrease compared to the pure OxD. The mass loss is divided into two consecutive processes related to the decomposition of OxD and 2-HPβCD. Of note, two endothermic peaks are associated with each melting point of the molecules. The decomposition process also exhibits a two-step pattern associated with the pure OxD and OxD:2-HPβCD inclusion complex decomposition.
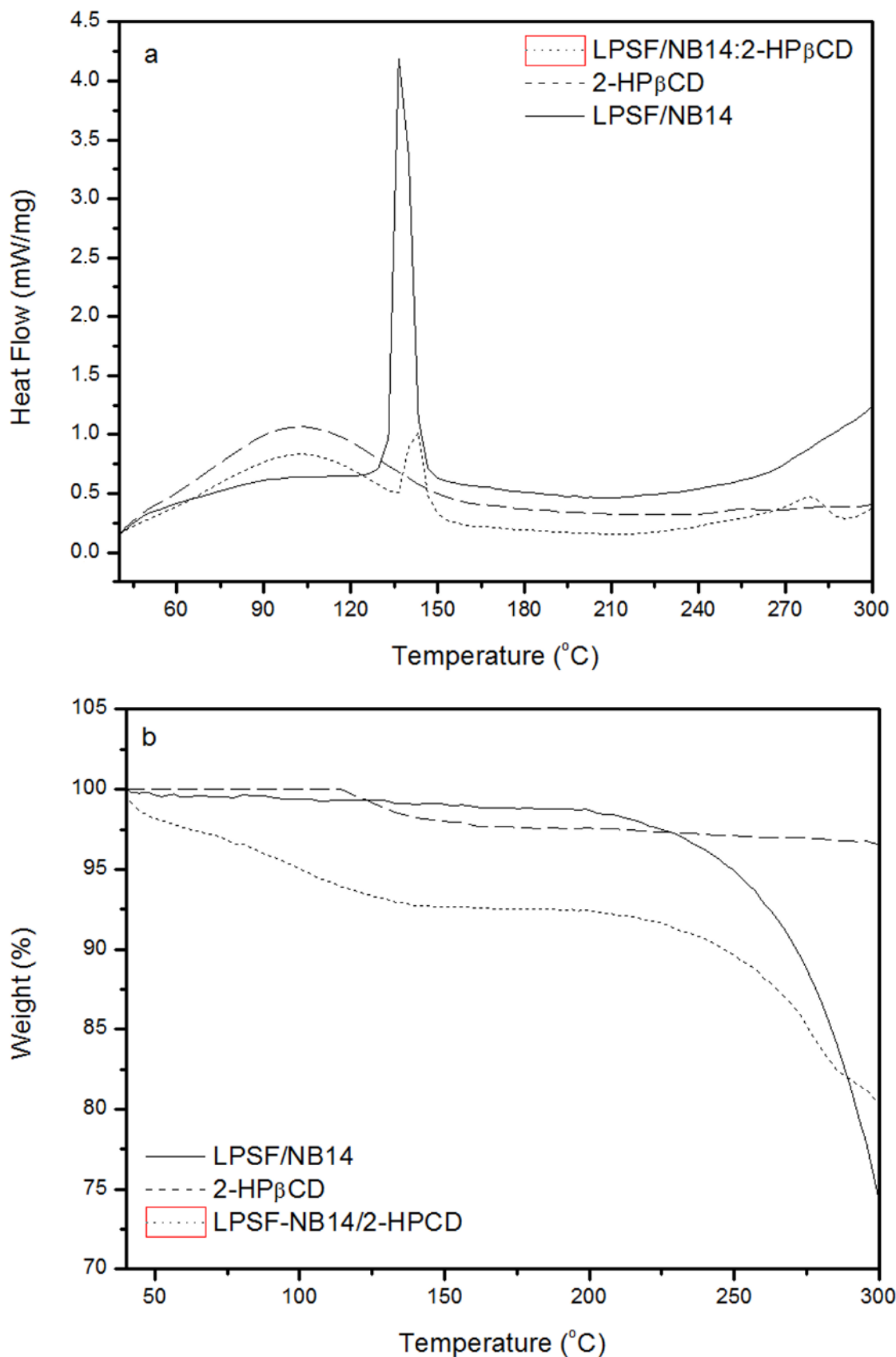
FIGURE 7 - DSC (a) and TG (b) curves of OxD and OxD:2-HPβCD inclusion complexes at 1:1 molar ratio.

Rafael R. Silva, Cézar A. C. Amorim, Maria C. A. Lima, Marcelo M. Rabello, Marcelo Z. Hernandes,
Moacyr J. B. M. Rêgo, Maira G. R. Pitta, Maria D. L. Oliveira, César A. S. Andrade

In vitro release study

Figure 8 shows the dissolution profiles of the OxD and OxD:2-HPβCD inclusion complex. The cumulative release rate of OxD:2-HPβCD obtained by the co-evaporation method was significantly higher than the physical mixture of OxD and OxD:2-HPβCD.

The dissolution was improved for OxD:2- HPβCD CE compared to OxD and OxD:2-HPβCD PM. The cumulative dissolution percentage for OxD:2-HPβCD CE and OxD:2-HPβCD PM was ~ 90% and 15.5%, respectively, during the first 15min. After, a plateau was observed for OxD:2-HPβCD CE. The differences observed in the dissolution profile of OxD and inclusion complex are related to the physical property and microenvironment around the molecules. The rapid release of OxD was attributed to the fact that β-CD improves the wettability of the inclusion complex in dissolution (Liu et al., 2013).
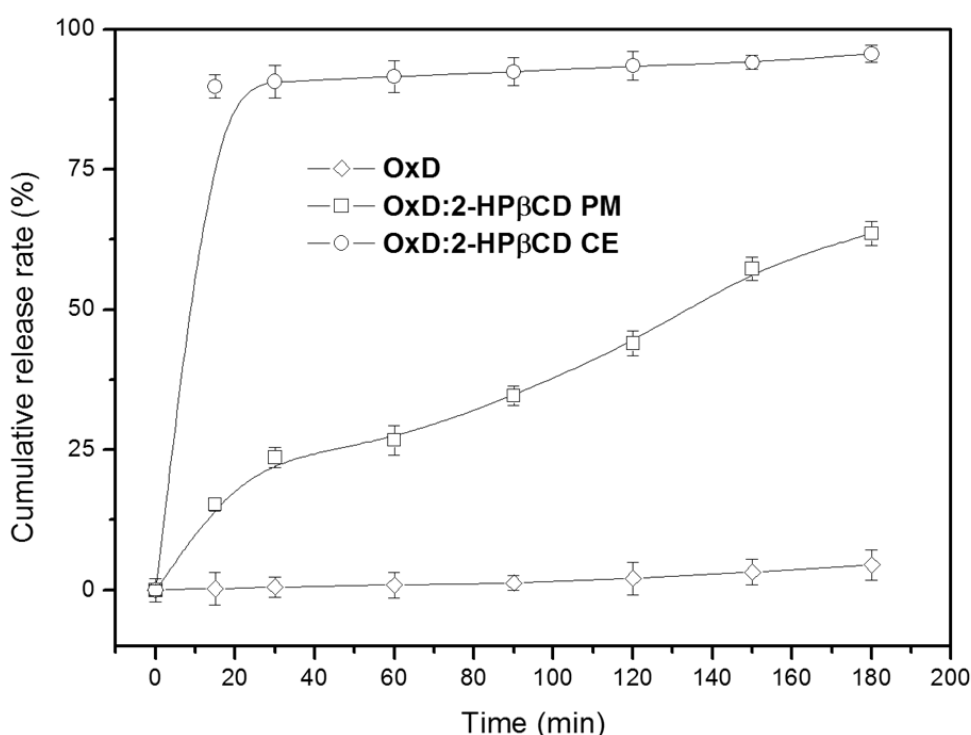
FIGURE 8 - In vitro release kinetics of OxD and OxD:2-HPβCD inclusion complex from a physical mixture (PM) and co-evaporation method (CE).

MTT Cytotoxicity Assay

The percentage of viable cells was obtained for six molar concentrations (1μM, 10 μM, 25 μM, 50 μM, 75 μM, and 100 μM) of OxD, 2-HPβCD, and inclusion complexes by using MTT assay (RPMI 1640 medium) (Figure 9). OxD cell viability was 95% (± 2.3%) for 1μM to 50μM. Pure 2-HPβCD and inclusion complexes showed cell viability of about 94% (± 3%) for all studied concentrations. Cyclodextrin shows specific cytotoxicity and is dose-dependent according to the involved cells (Sofian et al., 2014; Zhang et al., 2009). In general, concentrations > 25 μM are undesired for eventual in vivo tests, and therefore it is necessary to establish an optimal dose considering the amount used. The increment of the solubility of the OxD has been improved by using 2-HPβCD. In addition, 2-HPβCD and inclusion complexes showed less toxicity in normal cells.
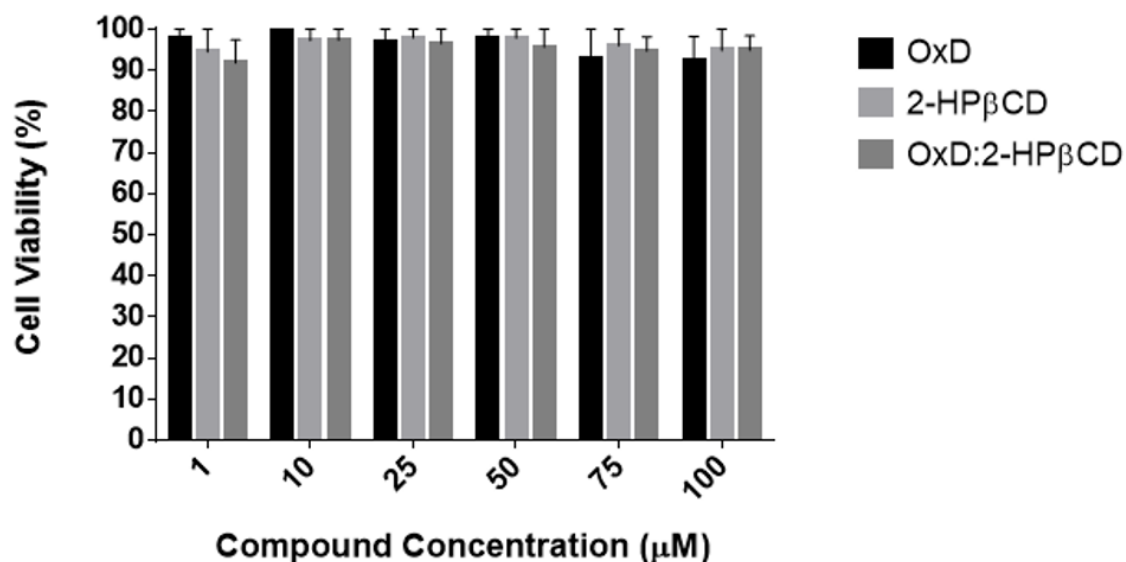
FIGURE 9 - Cytotoxicity of OxD and inclusion complexes toward PBMCs.

CONCLUSIONS

The molecular modeling studies showed stable intermolecular interactions between OxD and 2-HPβCD. The intermolecular energies and ^{1}H-NMR results of the inclusion complex also suggest a hydrogen bonding between guest and host molecules. The stability of inclusion complexes depends on intermolecular interactions such as Van der Waals forces and electrostatic and hydrophobic interactions. Our results demonstrated a solubility enhancement of OxD:2-HPβCD inclusion complex 20-fold more than pure OxD. The inclusion complexes show insignificant cytotoxicity in PBMCs viability. To the best of our knowledge, it is the first time that 2-HPβCD has been applied as an inclusion complex involving OxD. The proposed system could be used as a new oral delivery system for antitumor applications.

ACKNOWLEDGEMENTS

REFERENCES

Alves RJ, Fernandes DEAS, Souza FEM, Oliveira MC, Silvanos TC. 2014. N-substituted chiral aromatic oxazolidines, synthesis process, pharmaceutical composition and use: Google Patents.

Alvira E, Mayoral JA, García JI. Molecular modelling study of β-cyclodextrin inclusion complexes. Chem Phys Lett. 1997;271(1–3):178-184.

Bakhtiar R, Hop CE, Walker RB. Effect of cyclodextrins on the hydrolysis of an oxazolidine prodrug of (1R,2S)-(-)-ephedrine-cis-2-(4-methoxyphenyl)-3,   4-dimethyl-5-phenyloxazolidine. Rapid Commun Mass Spectrom. 1997;11(6):598-602.

Campos JF, Pereira MC, Sena WLB, Martins CGB, de Oliveira JF, Amorim CAC, et al. Synthesis and in vitro anticancer activity of new 2-thioxo-oxazolidin-4-one derivatives. Pharmacol Rep. 2017;69(4):633-641.

Cavalcanti IM, Mendonca EA, Lira MC, Honrato SB, Camara CA, Amorim RV, et al. The encapsulation of beta-lapachone in 2-hydroxypropyl-beta-cyclodextrin inclusion complex into liposomes: a physicochemical evaluation and molecular modeling approach. Eur J Pharm Sci. 2011;44(3):332-340.

Carvalho SG, Siqueira LA, Zanini MS, Matos APS, Quaresma CH, da Silva LM, et al. Physicochemical and in vitro biological evaluations of furazolidone-based β-cyclodextrin complexes in Leishmania amazonenses. Res Vet Sci. 2018;119:143-153.

Rafael R. Silva, Cézar A. C. Amorim, Maria C. A. Lima, Marcelo M. Rabello, Marcelo Z. Hernandes,
Moacyr J. B. M. Rêgo, Maira G. R. Pitta, Maria D. L. Oliveira, César A. S. Andrade

Challa R, Ahuja A, Ali J, Khar RK. Cyclodextrins in drug delivery: An updated review. AAPS PharmSciTech. 2005;6(2):E329-E357.

Choe HW, Park KS, Labahn J, Granzin J, Kim CJ, Buldt G. Crystallization and preliminary X-ray diffraction studies of alpha-cyclodextrin glucanotransferase isolated from Bacillus macerans. Acta Crystallogr D Biol Crystallogr. 2003;59(Pt 2):348-349.

Cirri M, Maestrelli F, Orlandini S, Furlanetto S, Pinzauti S, Mura P. Determination of stability constant values of flurbiprofen–cyclodextrin complexes using different techniques. J Pharm Biomed Anal. 2005;37(5):995-1002.

Dahiya S, Pathak K. Physicochemical characterization and dissolution enhancement of aceclofenac-hydroxypropyl beta-cyclodextrin binary systems. PDA J Pharm Sci Technol. 2006;60(6):378-388.

Fauziah CI, Zaibunnisa AH, Osman H, Aida WMW. Thermal analysis and surface morphology study of cholesterol: β-cyclodextrin inclusion complex. Adv Mater Res. 2013;812:221-225.

Gould S, Scott RC. 2-Hydroxypropyl-β-cyclodextrin (HP-β-CD): A toxicology review. Food Chem Toxicol. 2005;43(10):1451-1459.

Halgren TA. MMFF VI. MMFF94s option for energy minimization studies. J Comput Chem. 1999;20(7):720-729.

Hara T, Hirayama F, Arima H, Yamaguchi Y, Uekama K. Prominent solubilizing effect of 2-hydroxypropyl-β-cyclodextrin on a new thiazolidine derivative (FPFS-410) with antidiabetic and lipid-lowering activities through inclusion complex formation. J Inclusion Phenom Macrocyclic Chem. 2006;56(1):135-139.

Higuchi T, Connors KA. Phase-solubility techniques. Adv Anal Chem Instrum. 1965;4:117-212.

Lima MCA, Pitta MGR, Pitta IR, Pereira, MC, Amorim CAC, Rego MJBM, et al. Derivados 2-Tioxo-Oxazolidínicos-N-Substituídos potencialmente úteis na terapia anticâncer. Patent No. BR102015016060A2. 2015.

Liu H, Yang G, Tang Y, Cao D, Qi T, Qi Y, et al. Physicochemical characterization and pharmacokinetics evaluation of beta-caryophyllene/beta-cyclodextrin inclusion complex. Int J Pharm. 2013;450(1-2):304-310.

Loftsson T, Hreinsdóttir D, Másson M. Evaluation of cyclodextrin solubilization of drugs. Int J Pharm. 2005;302(1–2):18-28.

Mendonca EA, Lira MC, Rabello MM, Cavalcanti IM, Galdino SL, Pitta IR, et al. Enhanced antiproliferative activity of the new anticancer candidate LPSF/AC04 in cyclodextrin inclusion complexes encapsulated into liposomes. AAPS PharmSciTech. 2012;13(4):1355-1366.

Miletic T, Kyriakos K, Graovac A, Ibric S. Spray-dried voriconazole-cyclodextrin complexes: solubility, dissolution rate and chemical stability. Carbohydr Polym. 2013;98(1):122-131.

Ouyang D, Smith SC. Computational pharmaceutics: application of molecular modeling in drug delivery.1st ed. Wiley; Chichester. 2015.

O'Boyle NM, Banck M, James CA, Morley C, Vandermeersch T, Hutchison GR. Open Babel: An open chemical toolbox. J Cheminform. 2011;3(1):1-14.

Pandit N, Singla RK, Shrivastava B. Current updates on oxazolidinone and its significance. Int J Med Chem. 2012;2012:159285.

Piel G, Dive G, Evrard B, Van Hees T, de Hassonville SH, Delattre L. Molecular modeling study of beta- and gamma-cyclodextrin complexes with miconazole. Eur J Pharm Sci. 2001;13(3):271-279.

Rasheed A, Ashok Kumar CK, Sravanthi VVNSS. Cyclodextrins as drug carrier molecule: a review. Sci Pharm. 2008;76(4):567–598.

Saenger W, Jacob J, Gessler K, Steiner T, Hoffmann D, Sanbe H, et al. Structures of the common cyclodextrins and their larger analogues-beyond the doughnut. Chem Rev. 1998;98(5):1787-1802.

Savjani KT, Gajjar AK, Savjani JK. Drug solubility: importance and enhancement techniques. ISRN Pharm. 2012a;2012:195727.

Silva CV, Barbosa JA, Ferraz MS, Silva NH, Honda NK, Rabello MM, et al. Molecular modeling and cytotoxicity of diffractaic acid: HP-beta-CD inclusion complex encapsulated in microspheres. Int J Biol Macromol. 2016;92:494-503.

Sofian ZM, Shafee SS, Abdullah JM, Osman H, Razak SA. Evaluation of the cytotoxicity of levodopa and its complex with hydroxypropyl-ß-cyclodextrin (hp-ß-cd) to an astrocyte cell line. Malays J Med Sci. 2014;21(Spec Issue):6-11.

Songngam S, Sukwattanasinitt M, Siralertmukul K, Sawasdee P. A 5,7-dimethoxyflavone/hydroxypropyl-β-cyclodextrin inclusion complex with anti-butyrylcholinesterase activity. AAPS PharmSciTech. 2014;15(5):1189-1196.

Tiwari G, Tiwari R, Rai AK. Cyclodextrins in delivery systems: Applications. J Pharm BioAllied Sci. 2010;2(2):72-79.

Treib J, Baron JF, Grauer MT, Strauss RG. An international view of hydroxyethyl starches. Intens Care Med. 1999;25(3):258-268.

Trott O, Olson AJ. AutoDock Vina: improving the speed and accuracy of docking with a new scoring function, efficient optimization, and multithreading. J Comput Chem. 2010;31(2):455-461.

Wenz G. Cyclodextrins as building blocks for supramolecular structures and functional units. Angewandte Chemie Int. 1994;33(8):803-822.

Zhao Q, Ye Z, Su Y, Ouyang D. Predicting complexation performance between cyclodextrins and guest molecules by integrated machine learning and molecular modeling techniques. Acta Pharm Sin B. 2019;9(6):1241–1252.

Zhang WF, Zhou HY, Chen XG, Tang SH, Zhang JJ. Biocompatibility study of theophylline/chitosan/beta-cyclodextrin microspheres as pulmonary delivery carriers. J Mater Sci Mater Med. 2009;20(6):1321-1330.